2008 American Control Conference
Westin Seattle Hotel, Seattle, Washington, USA
June 11-13, 2008

Evaluation of Charge Drives for Scanning Probe Microscope Positioning Stages

Andrew J. Fleming[†]
School of Electrical Eng. and Computer Science
The University of Newcastle
Callaghan, NSW 2308, Australia

Kam K. Leang[‡]
Department of Mechanical Engineering
Virginia Commonwealth University
Richmond, Virginia, 23284-3015, USA

Abstract— **Due to hysteresis exhibited by piezoelectric actuators, positioning stages in scanning probe microscopes require sensor-based closed-loop control. Although closed-loop control is effective at eliminating non-linearity at scan speeds below 10Hz, it also severely limits bandwidth and contributes sensor-induced noise. The need for high-gain feedback is reduced or eliminated if the piezoelectric actuators are driven with charge rather than voltage. Charge drives can reduce hysteresis to less than 1% of the scan range. This results in a corresponding increase in bandwidth and reduction of sensor induced noise. In this work we review the design of charge drives and compare them to voltage amplifiers for driving lateral SPM scanners. The first experimental images using charge drive are presented.**

I. Introduction

A key component of Scanning Probe Microscopes (SPM's) [1] is the nanopositioning system required to manoeuvre the probe or sample. Piezoelectric actuators are universally employed in positioning systems due to their high stiffness, compact size and effectively infinite resolution. A major disadvantage of piezoelectric actuators however, is the hysteresis exhibited at high electric fields. This causes imaging artefacts in scanning probe microscopes. Techniques to eliminate this non-linearity include feedback, feedforward and image-based compensation, which are reviewed in references [2], [3] and [4].

The most popular technique for compensation in commercial scanning probe microscopes is sensor-based feedback using Proportional-Integral (PI) control. Such controllers are simple, robust to modeling error, and due to high loop-gain at low-frequencies, they effectively mitigate piezoelectric non-linearity. The foremost disadvantages of closed-loop control, however, are the cost, additional complexity, bandwidth limitations, and sensor-induced noise. In this work, the technique of charge control is evaluated for linearization of SPM positioning stages. The aim is to eliminate the requirement for feedback control and alleviate the associated problems.

Since the late 80's, it has been known that driving piezoelectric transducers with current or charge rather than voltage significantly reduces hysteresis [5]. Simply by regulating the current or charge, a five-fold reduction in hysteresis can be achieved [6]. Although the circuit topology of a charge or current amplifier is much the same as a simple voltage amplifier, the uncontrolled nature of the output voltage typically results in the load capacitor being linearly charged. Recent developments have eliminated low-frequency drift and permitted grounded loads, which are necessary in nanopositioning systems [7].

In the following section, charge drives are briefly reviewed, then applied to imaging experiments in Section III. A critical evaluation of charge drives for open- and closed-loop SPM applications is discussed in Sections IV and V, followed by conclusions.

II. Charge Drives

Consider the simplified diagram of a grounded load charge drive shown in Figure 1 [7]. The piezoelectric load, modeled as a capacitor and voltage source v_p, is shown in gray. The high-gain feedback loop works to equate the applied reference voltage v_{ref}, to the voltage across a sensing capacitor C_s. Neglecting the resistances R_L and R_s, at frequencies well within the bandwidth of the control loop, the load charge q_L is equal to

$$q_L = V_{ref} C_s, \tag{1}$$

i.e., the gain is C_s $Coulombs/V$. When connected to a capacitive load, the equivalent voltage gain is C_s/C_L.

As discussed in [7], the existence of R_L and R_s introduces error at low-frequencies. Essentially they draw charge away from the load and form a voltage feedback loop at DC and low-frequencies. This source of error can be eliminated

[†]Email: Andrew.Fleming@newcastle.edu.au
[‡]Email: kkleang@vcu.edu

978-1-4244-2079-7/08/$25.00 ©2008 AACC.

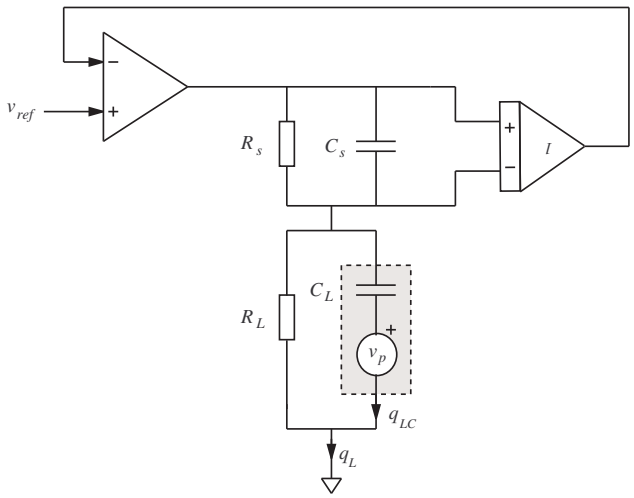

Fig. 1. DC accurate charge drive for grounded capacitive loads [7].

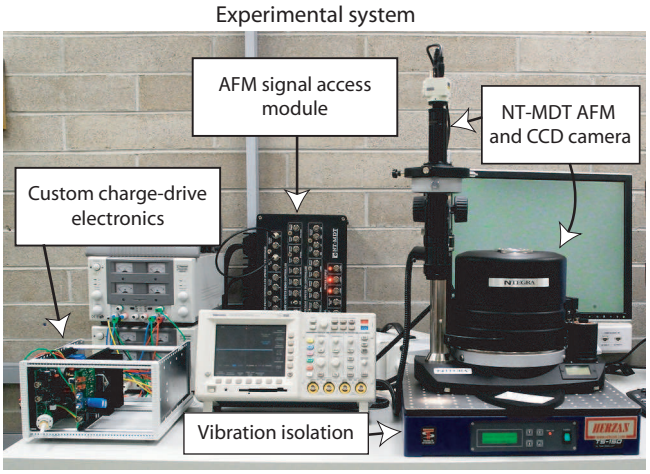

Fig. 2. A photograph of the experimental SPM system with charge drive electronics.

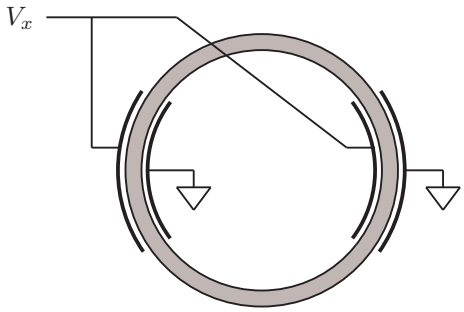

Fig. 3. Top view of the tube scanner. The x-axis electrodes are quartered on the inside and outside

by setting the ratio of the resistances equal to the ratio of capacitances. That is, by setting

$$\frac{R_L}{R_s} = \frac{C_s}{C_L} \tag{2}$$

the amplifier has a constant gain $C_s\ Coulombs/Volt$ over all frequencies.

Although the parallel resistances act to stabilize the voltage gain at low-frequencies, the amplifier now operates as a voltage source below $\frac{1}{2\pi R_L C_L}$ Hz and a charge drive above [7]. A consequence is that reduction of hysteresis only occurs at frequencies above $\frac{1}{2\pi R_L C_L}$ Hz. This cut-off frequency can be reduced by increasing R_L, however, a practical limit is imposed by the dielectric leakage of the transducer. Excessively high resistances also reduce immunity to drift resulting from current leakage to, or from, the high-impedance node between the two capacitors.

III. Experimental Imaging

Pictured in Figure 2, an NT-MDT Ntegra scanning probe microscope was retrofitted with a charge drive on the fast scanning x-axis. A signal access module allowed direct access to the scanner tube electrodes and reference signal. The charge gain was set to provide an equivalent voltage gain equal to the standard internal controller gain of 15. Accordingly, no modifications to the scan-controller or software interface were required.

The scanner is an NT-MDT Z50309cl tube scanner with 100 μm range. As shown in Figure 3, the tube has quartered internal and external electrodes that allow the scanner to be driven in a bridge configuration. Compared to the more popular grounded internal electrode configuration, the bridge configuration halves the required electrode voltage. In these experiments one pair of electrodes is grounded for simplicity.

During imaging, the AFM was operated in constant height, contact mode using a cantilever with spring constant 0.2 N/m. The lateral deflection of the piezo actuator was measured using capacitive sensors incorporated into the scanner assembly. A 1 Hz triangle wave was applied to develop scans of 5, 20 and 50 μm, corresponding to 5%, 20% and 50% of the maximum scan range. The scanner trajectories and tracking errors are plotted in Fig. 4. The maximum absolute errors for voltage and charge drive are compared in Table I.

The displacement non-linearity was only 2% in the 5 μm voltage-driven scan, this was marginally reduced by 54% to 0.86% using charge actuation. The linearity improvement for the 20 and 50 μm scans was marked. The voltage-driven non-linearity was 4.9% and 7.2% for the 20 and 50 μm ranges, this was reduced to 0.36% and 0.78% using charge,

	Absolute Scan Error		
Scan Range	Voltage	Charge	Reduction
5 μm	2.0 %	0.86 %	54 %
20 μm	4.9 %	0.36 %	93 %
50 μm	7.2 %	0.78 %	89 %

TABLE I

OPEN-LOOP SCAN ERROR WITH VOLTAGE AND CHARGE ACTUATION

a reduction 93% and 89%.

The AFM images of a 20 nm feature-height parallel calibration grating (3 μm pitch) are pictured in Fig. 5. Images were recorded by linearizing the y-axis with a capacitive sensor and driving the x-axis with voltage, then charge. 2% non-linearity is not discernable in the 5 μm scan. However, 4.9% and 7.2% non-linearity clearly distorts the 20 and 50 μm voltage-driven scans. In all three scans, where charge-driven non-linearity is less than 1%, the distortion is imperceptible. Reference lines in Figure 5 are superimposed on each image for comparision.

IV. CHARGE VERSUS VOLTAGE

In this section, advantages and drawbacks of charge drives are discussed for open-loop positioning applications.

A. Advantages

There are two motivating factors for the use of charge drives in scanning probe microscopes: reduction of hysteresis; and vibration compensation.

In Section III non-linearity of a tube scanner driven to half its full-scale range was measured at 7.2%. Subsequent images demonstrate that this magnitude of error is intolerable. Conversely, when driven with charge, scan error remains below 1% and is imperceptible in the images. Thus, while closed-loop control of voltage-driven AFM scanners is mandatory, charge drives eliminate this necessity. The follow-on benefits include zero sensor-induced noise, no controller imposed bandwidth limitations, simpler scanner design and lower cost.

In high-speed AFM systems [8] where feedback control is not feasible, the use of charge drives has the potential to significantly increase imaging performance. In addition to hysteresis reduction, damping of resonant modes can also be accomplished without the need for feedback. In reference [7], shunt-damping of scanner modes was accomplished by implementing a passive impedance in parallel with the scanner electrodes. The impedance is tuned to resonate with the transducers capacitance at the frequency of problematic modes. Greater than 20dB attenuation of the first lateral mode was demonstrated [7].

With hysteresis significantly reduced by charge drive, linear feedforward approaches [4] can also be implemented with high accuracy.

B. Disadvantages

The disadvantages of charge drives are the increased circuit complexity, voltage range reduction and necessity for gain tuning.

Although floating-load charge drives are similar to standard inverting voltage amplifiers, the grounded-load configuration in Figure 1 requires a high-performance differential buffer. The differential buffer requires high-input impedance, common-mode-range equal to the high-voltage supply and common-mode-rejection-ratio greater than 80dB over the bandwidth of the amplifier. These specifications are not met by available integrated devices but can be achieved with discrete designs, with increased circuit complexity. However, if the application does not require operation beyond 100 Hz, the differential buffer can be constructed easily with off-the-shelf parts.

As a consequence of the feedback signal's high common-mode-voltage, the grounded-load configuration generates more noise than a voltage amplifier of the same gain. This contrasts with the floating-load configuration that achieves less noise than a comparable voltage amplifier. In addition to amplifier noise, electromagnetic interference can contribute strongly to circuits with high-impedance nodes. In this regard the grounded-load configuration is superior as it is more easily shielded.

Due to the voltage drop across the sensing capacitor C_s, the output voltage range is limited by the maximum amplifier voltage minus the feedback voltage. This requires a slightly higher supply voltage to develop the same transducer displacement. For high-voltage devices greater than 100V, the maximum 10V drop across C_s is not significant. However, in lower voltage applications, this reduction may become significant as standard IC's are limited to between 36 and 50V. Simply increasing C_s and decreasing V_{ref} is an option for improving voltage range.

Aside from issues with the actual circuitry, the only significant difference between voltage and charge actuation is the need to adjust charge gain. At DC and low-frequencies, the voltage gain is fixed by the ratio of resistances R_L and R_s, these are easily interchanged or adjusted. To achieve the

(a) 5 μm Scan

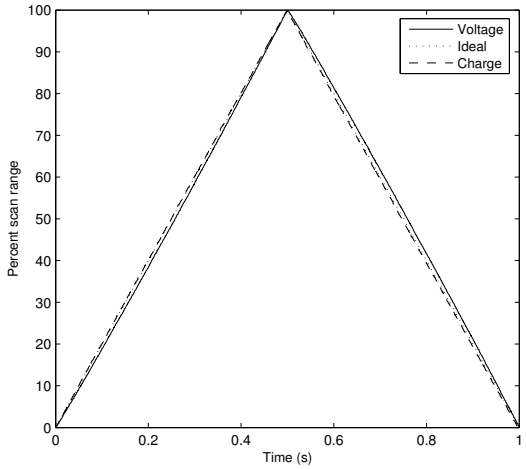

(b) 5 μm Scan Error

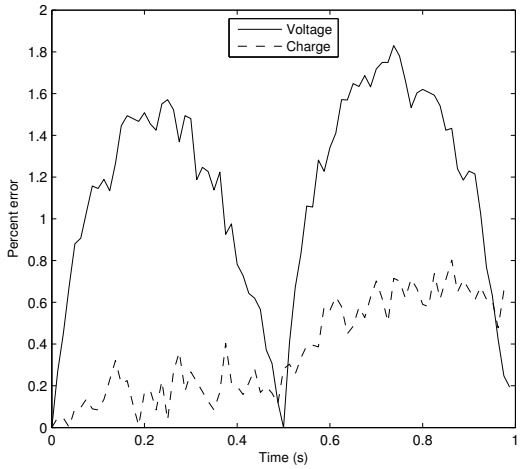

(c) 20 μm Scan

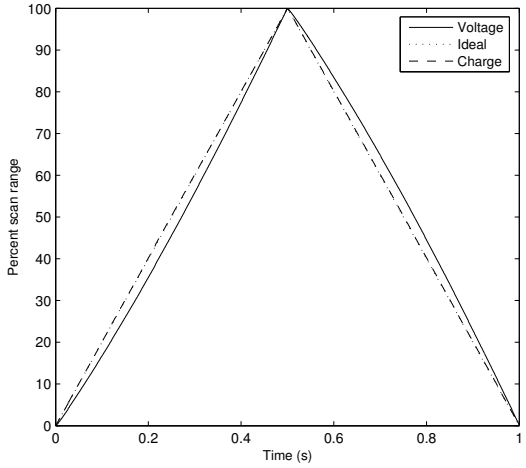

(d) 20 μm Scan Error

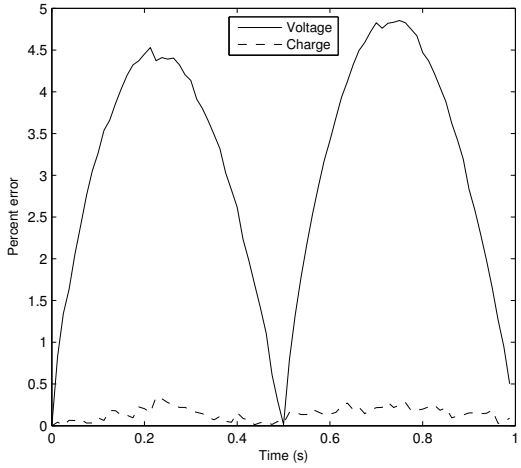

(e) 50 μm Scan

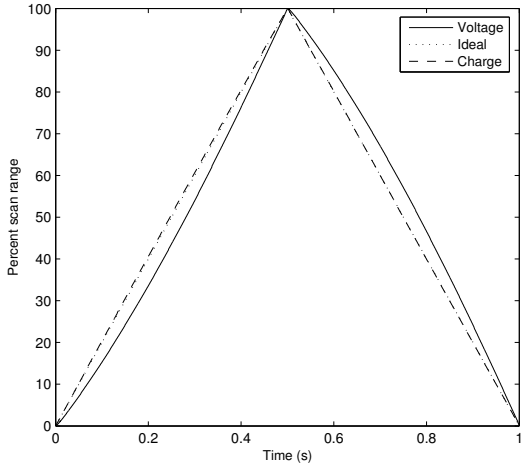

(f) 50 μm Scan Error

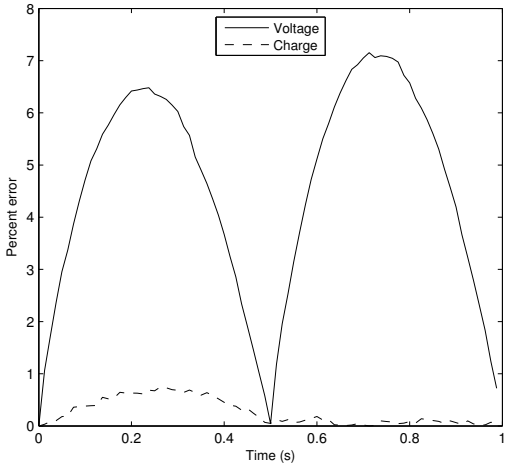

Fig. 4. The measured scanner deflection and percentage error for 5, 20 and 50 μm scans. The input was a 1 Hz triangle wave.

(a) Voltage drive 5×5 μm

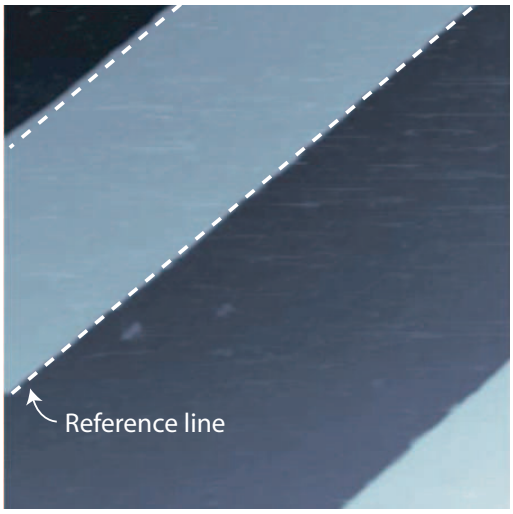

(b) Charge drive 5×5 μm

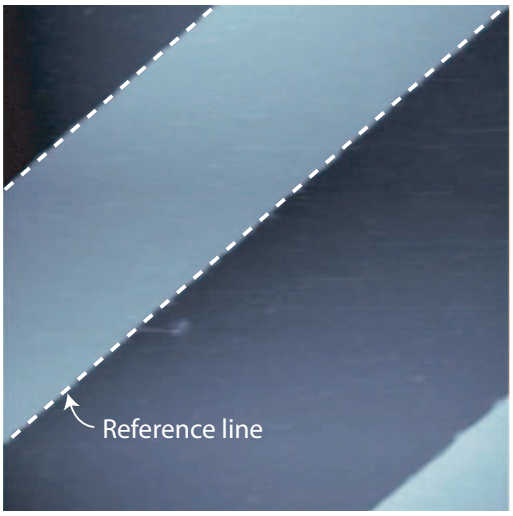

(c) Voltage drive 20×20 μm

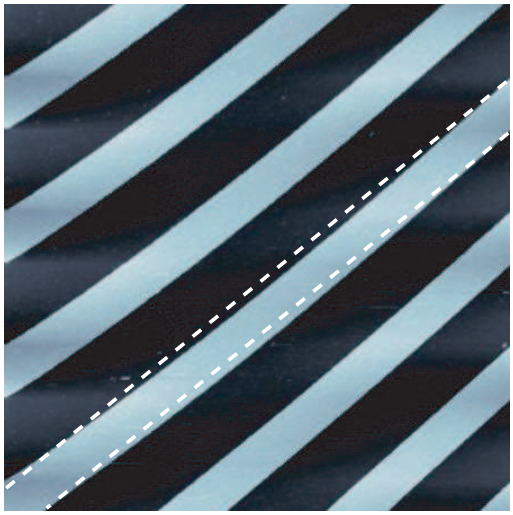

(d) Charge drive 20×20 μm

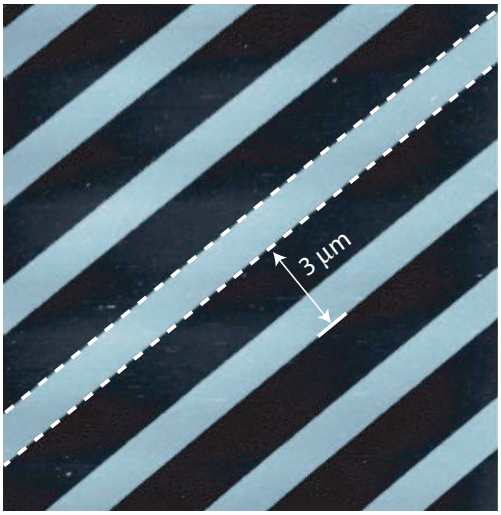

(e) Voltage drive 50×50 μm

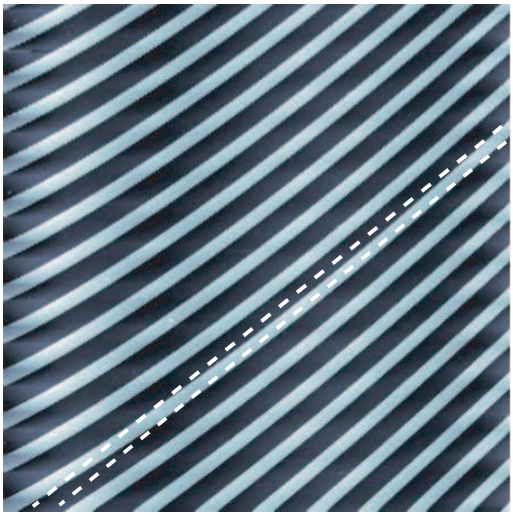

(f) Charge drive 50×50 μm

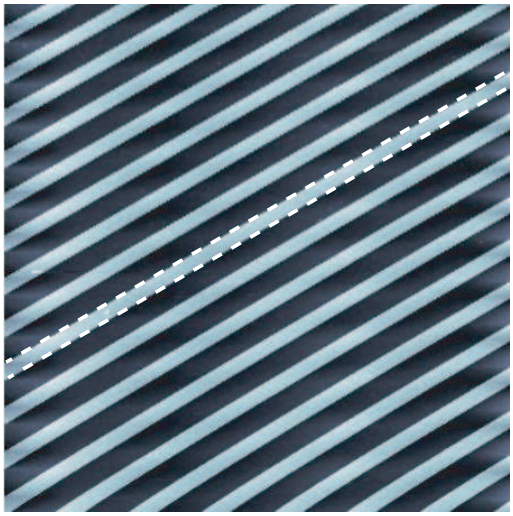

Fig. 5. A comparison of images recorded using voltage and charge actuation. The sample is a periodic calibration grating with 20 nm feature height

same gain at higher frequencies, C_s would need to be adjusted accordingly. This is impossible as variable capacitors of sufficient capacitance are not available. A better option is to select C_s larger than necessary, then add a gain α to the differential buffer, this allows a reduction of charge gain to that desired. After the charge gain is set, the resistance ratio R_L/R_s needs to be adjusted to $\alpha C_s/C_L$.

V. Impact on Closed-loop Control

At normal imaging speeds, *i.e.*, less than 10 Hz scan-rate, simple integral controllers with either damping controllers or notch filters for resonance compensation provide sufficient performance and are widely applied [9]. Over the frequency range where loop-gain is greater than 1, typically from DC to tens of Hz, the scanner displacement tracks additive sensor noise. Even with low-noise capacitive sensors (noise density $20pm/\sqrt{\text{Hz}}$), a controller bandwidth of 100 Hz results in greater than 1nm peak-peak noise. This precludes standard closed-loop scanners from achieving atomic resolution. The situation can be improved by dropping the controller bandwidth to 10 Hz. Although this provides the possibility for atomic resolution, the limited bandwidth restricts usage to the slow-scan axis only.

With charge control of the fast-axis, a sensor and wide bandwidth feedback loop are not required for linearization. Thus, no sensor induced noise is present. However, to eliminate thermal and mechanical drift, a slow feedback loop can be implemented. Although this provides rejection of DC and low frequency disturbance, the low bandwidth contributes minimal sensor induced noise.

VI. Conclusions

In this work, charge drives were evaluated for SPM positioning stages. The advantages are:

- Reduction of hysteresis to less than 1% of the scan range
- Straight-forward replacement for voltage amplifiers
- Compatible with sensor-less vibration control

Disadvantages include:

- Greater circuit complexity
- Requires tuning to set the gain
- Low frequency performance is limited by the transducer capacitance

Future work includes: developing circuits for bridged and asymmetric electrode configurations, high-speed operation, operation with stack actuators, and operation with high-power amplifiers.

Acknowledgements

This research was supported by the Australian Research Council (DP0666620) and the Centre for Complex Dynamic Systems and Control. Experiments were conducted at the Laboratory for Dynamics and Control of Nanosystems, University of Newcastle.

References

[1] E. Meyer, H. J. Hug, and R. Bennewitz, *Scanning Probe Microscopy*. Heidelberg, Germany: Springer, 2004.

[2] Q. Zou, K. K. Leang, E. Sadoun, M. J. Reed, and S. Devasia, "Control issues in high-speed afm for biological applications: collagen imaging example," *Asian Journal of Control*, vol. 6, no. 2, pp. 164–176, June 2004.

[3] D. Y. Abramovitch, S. B. Andersson, L. Y. Pao, and G. Schitter, "A tutorial on the mechanisms, dynamics, and control of atomic force microscopes," in *Proc. American Control Conference*, New York City, NY, July 2007.

[4] S. Devasia, E. Eleftheriou, and S. O. R. Moheimani, "A survey of control issues in nanopositioning," *IEEE Transactions on Control Systems Technology*, vol. 15, no. 5, pp. 802–823, September 2007.

[5] C. V. Newcomb and I. Flinn, "Improving the linearity of piezoelectric ceramic actuators," *IEE Electronics Letters*, vol. 18, no. 11, pp. 442–443, May 1982.

[6] P. Ge and M. Jouaneh, "Tracking control of a piezoelectric actuator," *IEEE Transactions on control systems technology*, vol. 4, no. 3, pp. 209–216, May 1996.

[7] A. J. Fleming and S. O. R. Moheimani, "Sensorless vibration suppression and scan compensation for piezoelectric tube nanopositioners," *IEEE Transactions on Control Systems Technology*, vol. 14, no. 1, pp. 33–44, January 2006.

[8] G. Schitter, K. J. strm, B. E. DeMartini, P. J. Thurner, K. L. Turner, and P. K. Hansma, "Design and modeling of a high-speed afm-scanner," *IEEE Transactions on Control Systems Technology*, vol. 15, no. 5, pp. 906–915, September 2007.

[9] K. K. Leang and S. Devasia, "Feedback-linearized inverse feedforward for creep, hysteresis, and vibration compensation in afm piezoactuators," *IEEE Transactions on Control Systems Technology*, vol. 15, no. 5, pp. 927–935, September 2007.